Biochimie xxx (2013) 1–10

Contents lists available at ScienceDirect

Biochimie

journal homepage: www.elsevier.com/locate/biochi

Research paper

Biochemical characterization of thioredoxin reductase from *Babesia bovis*

Erika L. Regner [a], Carolina S. Thompson [b], Alberto A. Iglesias [a], Sergio A. Guerrero [a], Diego G. Arias [a,*]

[a] *Instituto de Agrobiotecnología del Litoral (UNL–CONICET), Facultad de Bioquímica y Ciencias Biológicas, Paraje "El Pozo" CC 242, S3000ZAA Santa Fe, Argentina*

[b] *Estación Experimental Agropecuaria Rafaela, Instituto Nacional de Tecnología Agropecuaria, Rafaela, Santa Fe, Argentina*

ARTICLE INFO

Article history:
Received 16 July 2013
Accepted 6 November 2013
Available online xxx

Keywords:
Babesia
Eosin B
Nitrosoglutathione
Thioredoxin system
Glutathione disulfide

ABSTRACT

This paper addresses the identification, cloning, expression, purification and functional characterization of thioredoxin reductase from *Babesia bovis*, the etiological agent of babesiosis. The work deals with *in vitro* steady state kinetic studies and other complementary analyses of the thioredoxin reductase found in the pathogenic protist. Thioredoxin reductase from *B. bovis* was characterized as a homodimeric flavoprotein that catalyzes the NADPH-dependent reduction of Trx with a high catalytic efficiency. Moreover, the enzyme exhibited a disulfide reductase activity using DTNB as substrate, being this activity highly sensitive to inhibition by Eosin B. The thioredoxin reductase/thioredoxin system can reduce oxidized glutathione and *S*-nitrosoglutathione. Our *in vitro* data suggest that antioxidant defense in *B. bovis* could be supported by this enzyme. We have performed an enzymatic characterization, searching for targets for rational design of inhibitors. This work contributes to the better understanding of the redox biochemistry occurring in the parasite.

1. Introduction

Babesia bovis, a tick-borne haemoprotozoan parasite, causes severe and fatal infections in cattle at tropical and sub-tropical areas generating serious economic losses [1]. This protozoan, the causative agent of bovine babesiosis, belongs to the order Piroplasmida, phylum Apicomplexa. Similar to other members of this phylum, such as *Theileria* or its distant related organisms *Plasmodium* and *Babesia* undergo a complex life cycle involving both arthropod and mammalian hosts [2]. *Babesia* lives in an oxygen-rich environment in its mammalian host (erythrocytic stage), after which the parasite most likely is under the toxic effects of reactive species derived from oxygen (ROS) and/or from nitrogen (RNS). Thus, redox balance in parasites living in the host erythrocytes is an important biological parameter for the respective microorganism viability [3,4]. The elucidation of the *B. bovis* genome affords a key tool to identify the presence and operability of different metabolic pathways in the protist [5].

The thioredoxin (Trx) system is critical for the accurate maintenance of the intracellular redox state in many organisms. It plays an important role in different biological processes including the reduction of ribonucleotides, transcription control and hydrogen peroxide detoxification [6,7]. The system includes an NAD(P)H dependent disulphide oxidoreductase, namely Trx reductase (TrxR), and the Trx redox protein. Trxs are ubiquitous small proteins (10–12 kDa) having a conserved WCGPC catalytic site that undergoes reversible oxidation/reduction of the two Cys residues by means of TrxR at the expense of NAD(P)H [8]. TrxR is a member of the dimeric flavoenzymes family that catalyzes the transfer of electrons between pyridine nucleotides and disulfide/dithiol compounds, promoting the catalysis via FAD and a redox active disulfide.

Two distinct types of TrxR have been described [9,10]. Both are dimeric, although different respect to their amino acid sequences and catalytic mechanisms. One group includes low molecular weight (35 kDa subunit) TrxRs (L-TrxRs), as those found in bacteria, plants and fungi. The other group comprises bigger (55 kDa)

Abbreviations: TrxR, thioredoxin reductase; Trx, thioredoxin; GSSG, glutathione disulfide; GSNO, *S*-nitrosoglutathione; DTNB, dithio-nitrobenzoic acid; FAD, flavine adenine dinucleotide; FMN, flavine mononucleotide; Trx_{Red}, reduced thioredoxin; $TrxR_{Red}$, reduced thioredoxin reductase; H-TrxR, high molecular mass thioredoxin reductase.

* Corresponding author. Laboratorio de Bioquímica Microbiana, Instituto de Agrobiotecnología del Litoral (CONICET), Facultad de Bioquímica y Ciencias Biológicas, Universidad Nacional del Litoral (UNL), Santa Fe 3000, Argentina. Tel.: +54 342 4575221x131.

E-mail address: darias@fbcb.unl.edu.ar (D.G. Arias).

0300-9084/$ – see front matter © 2013 Elsevier Masson SAS. All rights reserved.
http://dx.doi.org/10.1016/j.biochi.2013.11.002

proteins, namely H-TrxRs, mainly localized in insects and mammals [9,10]. Between protozoa, the Trx system was extensively studied in *Plasmodium falciparum*. This parasite has an H-TrxR, which functionality is important for controlling the redox balance [11,12]. Instead, the enzymatic system has not been studied in *Babesia* spp; although in recent years a 2-Cys peroxiredoxin (*Bbo*TPx-1) was characterized in *B. bovis* as an important component with functional dependence on the Trx network [13]. Herein, we report the recombinant expression, purification and biochemical characterization of a classic Trx (with a typical WCGPC redox motif) and TrxR from *B. bovis*, analyzing the properties of the proteins in the context of their function in the redox metabolism of the parasite.

2. Materials and methods

2.1. Materials

Bacteriological media components were from Britania Laboratories (Buenos Aires, Argentina). All other reagents and chemicals were of the highest quality commercially available (Sigma–Aldrich and Merck).

2.2. Data bases

The following databases were used: NCBI GenBank™ Data Base (http://www.ncbi.nlm.nih.gov/genbank/), Sanger Center (http://www.sanger.ac.uk) and PiroplasmaDB genomics resources, a EupathDB project (http://piroplasmadb.org/piro/).

2.3. Preparation of S-nitrosoglutathione

S-nitrosoglutathione (GSNO) was prepared as previously described by nitrosation of GSH under acid conditions [14]. Briefly, equal volumes of glutathione (200 mM) and sodium nitrite (200 mM) were incubated in the presence of 10 mM HCl on ice for 30 min. GSNO was stabilized by addition of 1 mM EDTA at pH 7.0. GSNO was freshly prepared and stored on ice in the dark. The concentration of GSNO was estimated by measuring absorbance at 332 nm, using the absorption coefficient of 0.92 mM^{-1} cm^{-1} [14].

2.4. Bacteria and plasmids

Escherichia coli Top 10 cells (Invitrogen) and *E. coli* BL21 (DE3) (Novagen) were utilized in routine plasmid construction and expression experiments, respectively. The vector pGEM-T Easy (Promega) was used for cloning and sequencing purposes. The expression vector used was pET28a vector (Novagen).

2.5. Protozoa and culture procedure

In vitro cultures *B. bovis* strains were multiplied *in vitro* using a microaerophlic stationary-phase culture method. Briefly, the basic medium (BM) consisted of M199 (Gibco®) supplemented with 0.1 g/l penicillin, 0.16 g/l streptomycin, 2.2 g/l $NaHCO_3$, and 4.25 g/l HEPES and enriched with 40% normal bovine serum (v/v). The complete medium (CM) included 5–10% (v/v) normal bovine erythrocytes. Cultures were incubated at 37 °C under 5% CO_2 in air or under 5% O_2, 5% CO_2 and 90% N_2. BM was replaced every 24 h, and a variable proportion of parasitized CM was replaced by normal CM after 48, 72 or 96 h (subculture) [15].

2.6. Molecular cloning of trxr and trx from B. bovis

RNA extraction from *B. bovis* (strain S2P) merozoites was performed using TRIzol® reagent (Invitrogen). Oligonucleotide primer pairs utilized for PCR amplification were designed from reported sequences (PiroplasmadDB – http://piroplasmadb.org/piro/). The *bbotrx* gen (BBOV_II003650) was amplified by RT-PCR using RNA from *B. bovis* merozoites, M-MVL reverse transcriptase (Promega) and Taq DNA polymerase (Thermo Scientific). The forward primer was designed to introduce a *Bam*HI restriction site (5′-GGATCCATGGTGAAACAAATTGCT-3′) and the reverse primer a *Hind*III restriction site (5′-AAGCTTTTATACATTCTTGTCAATAGCG-3′). The PCR product was subsequently purified and ligated into the pGEM-T Easy vector (Promega) to facilitate further work. The fidelity and correctness of the sequence was confirmed by complete sequencing.

Attempts for the amplification of the *bbotrxr* gene (BBOV_I002190) were performed by RT-PCR using RNA from *B. bovis* merozoites using the designed primers: 5′-GGATCCATGAGGCGAAGGACTCCTTT-3′ and 5′-CTCGAGCTAACCGCAACGACCACCAC-3′. Alternatively, the *bbotrxr* gene was synthesized *de novo*, optimizing the codon preference for expression in *E. coli* (Bio Basic Inc., Canada) flanked by the restriction sites *Bam*HI and *Hind*III and cloned in pUC59 plasmid. In addition, based on predictive data concerning the possible existence of an N-terminal signal peptide, we generated a truncated version of *bbotrxr* gene (1_150del*bbotrxr*) by PCR using the optimized *bbotrxr* sequence as template. The forward primer was designed to introduce a *Bam*HI restriction site (5′-GGATCCATGTCTAACACCAACAACTCCG-3′) and the reverse primer a *Hind*III restriction site (5′-AAGCTTTTAACCGCAACGACCACCAC-3′). The PCR product was subsequently purified and ligated into the pGEM-T Easy vector (Promega) to facilitate further work. The fidelity and correctness of the sequence was confirmed by complete sequencing. The pUC59/*bbotrxr*, pGEM-T Easy/1_150del*bbotrxr* and pGEM-T Easy/*bbotrx* plasmids were digested with *Bam*HI and *Hind*III enzymes and ligated to the pET28a (Novagen) vector. DNA manipulation, *E. coli* culture, and transformation were performed according to standard protocols.

2.7. Expression and purification

Single colonies of *E. coli* BL21 (DE3) transformed with the respective recombinant plasmid were selected. Overnight cultures were diluted 1/100 in fresh medium (LB broth supplemented with 50 μg/ml kanamycin) and grown under identical conditions to exponential phase, OD600 of 0.6. The expression of recombinant proteins was induced with 0.25 mM IPTG, followed by incubation at 28 °C. After 16 h the cells were harvested and stored at −20 °C. Purification of recombinant *Bbo*Trx and *Bbo*TrxR was carried out by chromatography onto a Ni^{2+}–IDA–agarose resin (Invitrogen). Briefly, the bacterial pellet was resuspended in binding buffer (20 mM Tris–HCl, pH 7.5, 400 mM NaCl, 15 mM imidazole) and disrupted by sonication. The lysate was centrifuged (10,000 *g*, 30 min) to remove cell debris and the resultant crude extract was loaded onto the chromatographic column that had been equilibrated with binding buffer. The column was washed with 10 column volumes of the same buffer, after which the recombinant protein was eluted with elution buffer (20 mM Tris–HCl, pH 7.5, 400 mM NaCl, 300 mM imidazole). Active fractions were pooled and stored at −80 °C with 10% glycerol (Merck). Under the specified storage conditions, the recombinant proteins were stable for at least 4 months. His-tagged *E. coli* Trx (*Eco*Trx) was obtained from *E. coli* BL21 (DE3) cells transformed with the commercial pET32a plasmid (Novagen) and it was purified by the same procedure utilized for the proteins from *B. bovis*.

2.8. Protein methods

SDS-PAGE was carry out using the Bio-Rad minigel equipment, basically according to previously described methods [16]. Protein

Please cite this article in press as: E.L. Regner, et al., Biochemical characterization of thioredoxin reductase from *Babesia bovis*, Biochimie (2013), http://dx.doi.org/10.1016/j.biochi.2013.11.002

concentrations were determined by the method of Bradford [17], utilizing BSA as standard.

2.9. Determination of the molecular mass by gel filtration chromatography

The determination of the native molecular mass of proteins was performed by gel filtration chromatography in a Superdex 200 HR Tricorn column (GE). The calibration curve was constructed using the logarithm of the molecular mass (log MM) of standard proteins vs. the respective distribution coefficient (K_{av}) for: thyroglobulin (669 kDa), ferritin (440 kDa), aldolase (158 kDa), conalbumin (75 kDa), ovalbumin (43 kDa), carbonic anhydrase (29 kDa), ribonuclease A (13.7 kDa) and aprotinin (6.5 kDa) (Gel Filtration Calibration Kit – GE).

2.10. Flavin determination

Purified *Bbo*TrxRΔ50N was boiled in the dark for 10 min and centrifuged to remove the denatured protein. The cofactor of the protein was visualized by resolving the supernatant at room temperature and in the dark by thin layer chromatography (TLC) on silica sheets 25 TLC ALUMINIUM plates (Merck). The mobile phase was a solution of butanol/acetic acid/water (12:3:5). The chromatogram was analyzed by fluorescence with the *Typhoon* scanner (GE Healthcare). A solution of commercial FAD and FMN was used as a standard. After identification of the flavin, its concentration was quantified spectrophotometrically using the molar extinction coefficient at 450 nm of 11.3 mM^{-1} cm^{-1} [18].

2.11. BboTrxRΔ50N and Trx system kinetic analysis

All enzymatic assays were performed spectrophotometrically at 30 °C using a Multiskan Ascent one-channel vertical light path filter photometer (Thermo Electron Co.). The general assay medium contained 100 mM potassium phosphate, pH 8.0, and 2 mM EDTA. In all the cases, the final volume was of 50 μl.

Activity for 5,5′-dithiobis (2-nitrobenzoic acid) (DTNB) reductase was measured by monitoring the production of thionitrobenzoate at 405 nm after complementing the assay medium with 0.1 mM NADPH, 0.02–2.5 mM DTNB, and 0.14–18 nM *Bbo*TrxRΔ50N. Activity was calculated using the molar extinction coefficient at 405 nm of 13.6 mM^{-1} cm^{-1} and considering that 1 mol of NADPH yields 2 mol of thionitrobenzoate.

TrxR activity was measured by monitoring NADPH oxidation at 340 nm with the addition to the assay medium of 0.1 mM NADPH, 0.1 mM human insulin, 0.4–50 μM Trxs, and 0.14–18 nM *Bbo*TrxRΔ50N. Kinetic of NADPH oxidation by *Bbo*TrxR was monitored with the *Bbo*Trx-mediated reduction of DTNB, following an increase in absorbance at 405 nm. Typically, 500 μM DTNB, 20 μM *Bbo*Trx, 18 nM *Bbo*TrxR and 0.5–50 μM NADPH was used in presence of a system of NADPH regeneration (1 mM glucose-6-phosphate and 5 mg ml^{-1} glucose-6-phosphate dehydrogenase).

Assay for GSNO or GSSG (each in the range 7.25–1000 μM) reduction was assayed using these species as final electron acceptors at variable concentrations, 0.01–1 μM *Bbo*TrxRΔ50N, 0.1 mM NADPH, and different concentrations (0–8 μM) of *Bbo*Trx. The reactions were started by adding GSNO or GSSG. This assay was followed by the absorbance decrease at 340 nm.

Inhibition of *Bbo*TrxRΔ50N by variable concentrations (8–1000 μM) of $NADP^+$ was evaluated at three levels of NADPH (12.5, 25 and 50 μM). For determination of *Ki* values the data were plotted according to Dixon [19].

Eosin B was tested as an enzyme inhibitor by monitoring the reduction of DTNB at 405 nm. In each series of experiments six inhibitor concentrations were used: 0, 2.5, 5, 25, 50 and 100 μM. The DTNB concentrations in the assay ranged from 40 to 5000 μM.

All kinetic parameters were acquired by fitting the data with a nonlinear least-squares formula and Michaelis–Menten equation using the program Origin. Kinetic constants are the mean of at least three independent sets of data, and they were reproducible within ±10%.

2.12. Stress resistance assays

For disk inhibition assays recombinant *E. coli* cells were grown overnight at 37 °C in LB broth containing kanamycin (50 μg ml^{-1}), then diluted 1/100 in LB medium and further incubated at 37 °C until a final optical density of 0.5. These cells were grown in the presence of 0.1 mM IPTG for another 4 h and then poured into plates with addition of IPTG and kanamycin. A sterilized filter disk (6 mm in diameter), previously soaked with 10 μl of either 20 or 200 mM diamide, and was placed in the middle of the plate. The plates were overnight incubated at 37 °C.

3. Results

3.1. Cloning, purification, and characterization of classic Trx and TrxR from B. bovis

Using the *B. bovis* genome database (PiroplasmaDB) we identified two ORFs related with classic components of the Trx system: BBOV_II003650 and BBOV_I002190. The reported BBOV_II003650 (namely *bbotrx* gene) sequence codes for a putative Trx protein (*Bbo*Trx) that has 105 amino acids, a molecular mass of 11.4 kDa and a calculated pI of 6.7. The deducted amino acid sequence contains the WCGPCK motif that has been identified as the redox active site in classic Trxs [20,21]. Concerning the BBOV_I002190 (namely *bbotrxr*) gene, it encodes a protein (*Bbo*TrxR) of 559 amino acids with a predicted molecular mass of 60.7 kDa. *Bbo*TrxR is similar in size to other members of H-TrxRs [21–23], and its amino acid sequence shows identities of 38% and 45% with TrxRs from bovine and *P. falciparum*, respectively (Fig. 1). Furthermore, in PiroplasmaDB we found another ORF for a possible non-classical Trx (BBOV_III011040). This putative protein has the WCKPC motif as active redox site. In this paper we focus on the characterization of the classical Trx, pending the functional study of other putative Trxs occurring in this parasite.

To further seek for the functionality of the *Bbo*TrxR/*Bbo*Trx system, we constructed expression vectors to recombinantly express Trx and TrxR, each one fused to an N-term His-tag to reach high purification degree (Fig. 2). On the one hand, we easily amplified the *bbotrx* gene by RT-PCR from RNA obtained from *B. bovis* (strain S2P) merozoites, cloning it into a pET28a (Novagen) vector as described under "Materials and Methods". The recombinant *Bbo*Trx, was chromatographically purified onto a Ni^{2+}-affinity resin to reach electrophoretic homogeneity (Fig. 2A). The molecular mass revealed for this protein, 12 kDa, agrees with the size expected from the respective sequence. Conversely, using the same procedure we failed in the amplification of the BBOV_I002190 gene, even when different experimental conditions were tested. In order to overcome this problem, the gene was synthesized *de novo* (Bio Basic Inc.) with optimization for the codon usage of the host expression organism *E. coli*. The expression of the synthesized *bbotrxr* gene rendered all of the recombinant protein in inclusion bodies, with no detection of activity in soluble fractions in crude extracts (Fig. 2B). The system showed recalcitrant to express *Bbo*TrxR in a soluble form after several variants experimented for the expression, which leads us to revisit the protein primary structure. By *in silico* analysis using SOSUI, TargetP and SignalP

Please cite this article in press as: E.L. Regner, et al., Biochemical characterization of thioredoxin reductase from *Babesia bovis*, Biochimie (2013), http://dx.doi.org/10.1016/j.biochi.2013.11.002

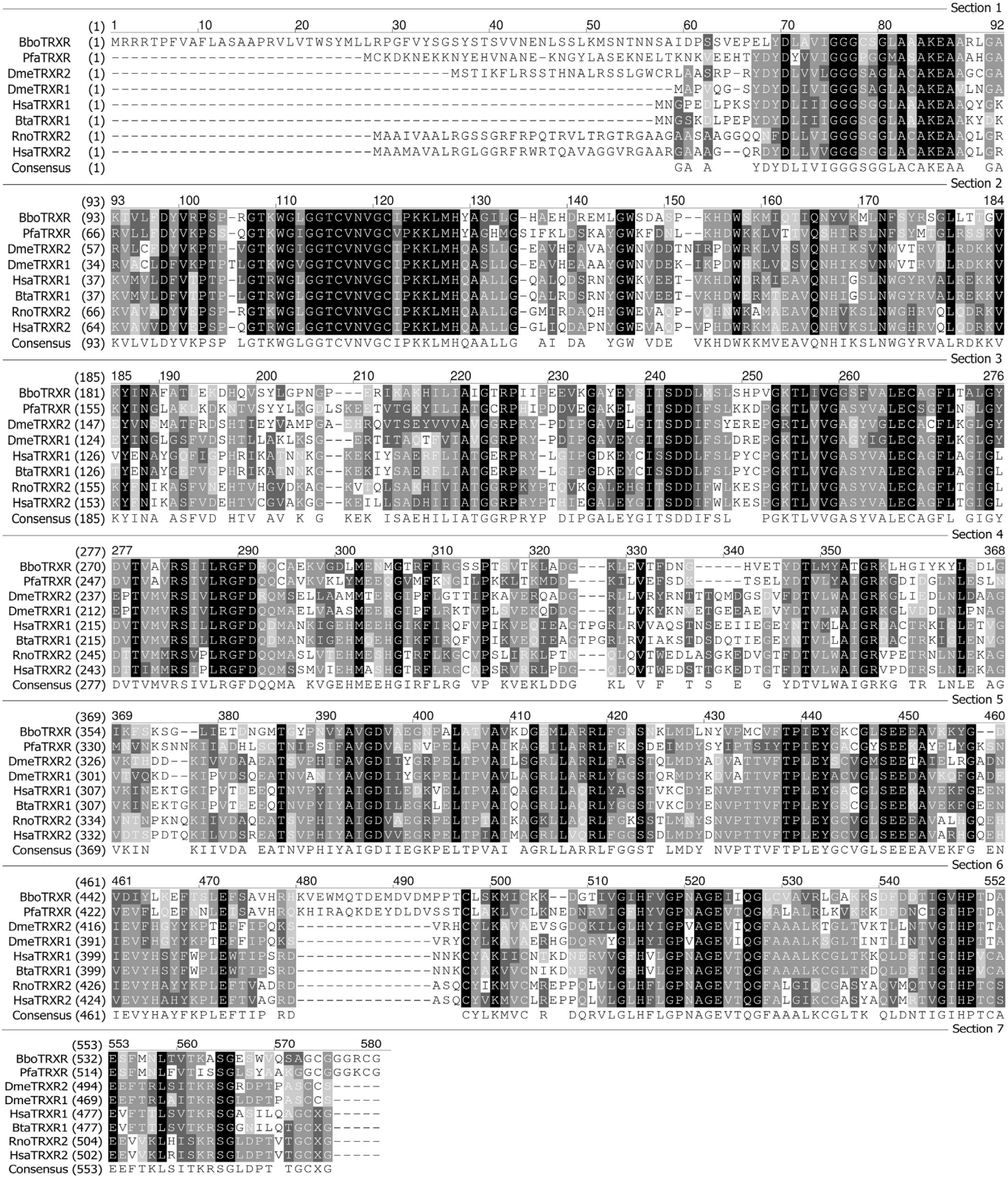

Fig. 1. Amino acids sequence alignment of *Bbo*TrxR with TrxR homologues. *Plasmodium falciparum* TrxR (CAA60574), *Drosophila melanogaster* TrxR 2 (NP_524216.1), *Drosophila melanogaster* TrxR 1 (NP_511082.2), *Homo sapiens* TrxR 1 (AAB35418.1), *Bos taurus* TrxR 1 (AAC13914.1), *Rattus norvegicus* TrxR 2 (AAD13801.1) and *Homo sapiens* TrxR 2 (AAD25167.1). Each individual sequence is numbered accordingly.

Please cite this article in press as: E.L. Regner, et al., Biochemical characterization of thioredoxin reductase from *Babesia bovis*, Biochimie (2013), http://dx.doi.org/10.1016/j.biochi.2013.11.002

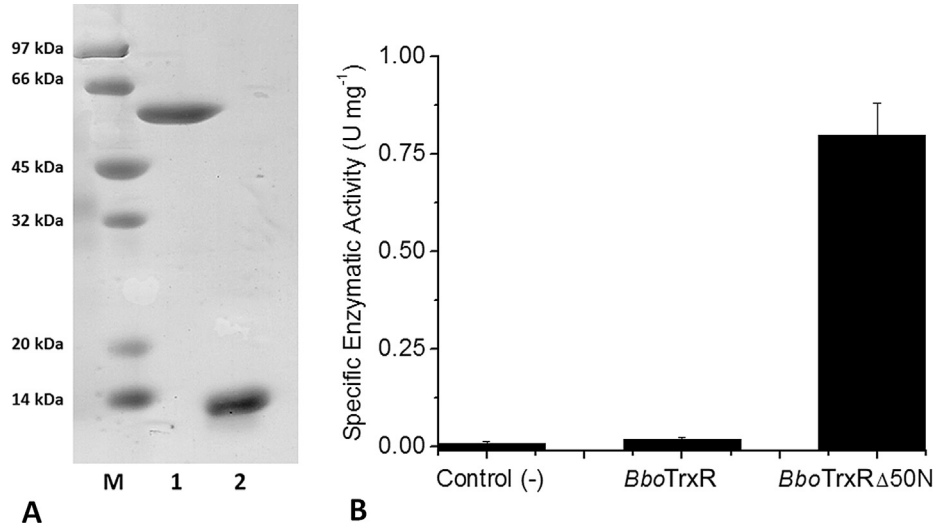

Fig. 2. Expression and purification of recombinant *Bbo*Trx system. A – Electrophoretic analysis of purified recombinant proteins. The proteins were defined by 15% (w/v) SDS-PAGE and stained with Coomassie blue. *M* indicates molecular mass markers. *Lane 1*, *Bbo*TrxRΔ50N; *lane 2*, *Bbo*Trx. B – DTNB reductase activity determinate in soluble recombinant *E. coli* extracts after induction with IPTG. Control (–): transformed *E. coli* with pET28 plasmid, *Bbo*TrxR: transformed *E. coli* with pET28/*Bbo*TrxR plasmid (full ORF) and *Bbo*TrxRΔ50N: transformed *E. coli* with pET28/*Bbo*TrxRΔ50N plasmid (truncated ORF).

servers it was determined that the protein sequence deducted from the *bbotrxr* gene contains an N-terminus (34, 44, and 34 amino acids long, respectively) with high predictive potential of mitochondrial signal peptide. The envisaged extension of the signal peptide agrees with what is depicted in Fig. 1, where the apparition of domains related with TrxR function is clear after the first 60 residues in the deduced sequence of *Bbo*TrxR. Considering all this information, we engineered the synthesized *bbotrxr* entire gene to obtain a truncated (1_150del*bbotrxr*) version coding for a shorter protein (*Bbo*TrxRΔ50N) starting at the Met^{51} of the ORF established from BBOV_I002190 (see Fig. 1). This truncated version was expressed as a soluble protein that could be purified to high degree, as judged by SDS-PAGE analysis (Fig. 2A), and that exhibited disulfide reductase activity (Fig. 2B).

We performed experiments to seek if, besides the *in vitro* activity exhibited by *Bbo*TrxRΔ50N (Fig. 2B), this truncated construct of the protein can be functional *in vivo*. In these experiments we used a well-known strong oxidant (diamide, which induce oxidative stress [24]) doing disk inhibition assays to test if *Bbo*TrxRΔ50N expression could protect *E. coli* cells against oxidative damage. As shown in Fig. 3, inhibition rings were observed either in the presence of 20 or 200 mM diamide, but *Bbo*TrxRΔ50N-expressing *E. coli* cells underwent less growth arrest than the control (pET28 transformed *E. coli* cells). These results support the *in vivo* functionality of the truncated *Bbo*TrxRΔ50N protein by conferring the bacterium cells enhanced tolerance to diamide-mediated oxidative damage.

3.2. Structure and kinetic properties of BboTrxRΔ50N

The absorption spectrum of oxidized *Bbo*TrxRΔ50N exhibited a maximal at 380 and 460 nm (Fig. 4A), typical of the flavoprotein family members [4,20,25], although it lacks the characteristic shoulder at 480 nm. As shown in Fig. 4A (and its inset), aerobic redox titration with NADPH caused a decrease in the absorbance at 460 nm and an increase at 560 nm. The inset in Fig. 4A shows an equivalent point for both titrations at a ratio NADPH:TrxR of 1. As described elsewhere [26–28], the absorbance at 460 nm corresponds to the reduction of the flavin prosthetic group in *Bbo*TrxR, while the absorbance at 560 nm indicates the formation of a thiolate-flavin charge–transfer complex. In most flavoproteins the cofactor is tightly but not covalently bound and this seems to be the case for *Bbo*TrxRΔ50N, as a bright yellow compound was released after boiling the purified protein for 10 min. The resulting prosthetic group was identified as FAD by TLC (Fig. 4B). In addition, the purified *Bbo*TrxRΔ50N eluted as a protein of ~100 kDa in gel filtration chromatography (data no shown), this suggesting that the enzyme forms a homodimeric structure in its native (active) state. The latter is in agreement with previous reports on TrxR from other sources [8,21].

*Bbo*TrxRΔ50N showed active as NADPH-dependent disulfide reductase, using DTNB as substrate (Fig. 5) and it was also able to reduce both *Bbo*Trx and the ortholog protein from *E. coli* (*Eco*Trx) (Fig. 6). This activity exhibited a maximum at pH 8.0 in 100 mM phosphate buffer and 30 °C (Fig. 7). Table 1 shows the kinetic parameters determined for NADPH and the disulfide substrates. No activity was detected when NADH (in equivalent concentration) was used instead of NADPH, a result that is consistent with previous reports concerning the enzymatic behavior of H-TrxRs [21,29,30]. In addition, no substrate inhibition was observed at high (up to 100 μM) NADPH concentrations (see Fig. 5). Results in Table 1 indicate that *Bbo*TrxRΔ50N exhibits a high affinity toward NADPH ($Km = 1.3 \pm 0.2$ μM), as well as a high catalytic efficiency ($k_{cat} \cdot Km^{-1}$) for reducing both Trxs (although being higher for *Bbo*Trx) (Fig. 6 and Table 1). These values are practically in the same order of magnitude than the parameters reported for malarial TrxR, and they are similar to those determined for H-TrxRs from other species [4,8,20,25].

Alternatively, different compounds were evaluated as possible acceptor substrates of *Bbo*TrxRΔ50N. In our hands, the recombinant enzyme exhibited neither oxidase activity (O_2 as final electron acceptor), nor any kind of reaction with lipoamide, dihydroascorbic acid, selenite, GSSG or cysteine (up to 2 mM, data not shown). Clearly, *Bbo*TrxR shows similar features than those found for other non-selenocysteine-containing H-TrxRs. On the contrary, the enzyme from mammalian cells has a C-terminal SeCys-containing domain that permits the reduction of a large spectrum of substrates [27,31,32].

3.3. GSNO and GSSG reduction by the BboTrxR/BboTrx system

GSNO represents an important transport form of nitric oxide (NO) in biological systems and it has been shown to be a substrate

Please cite this article in press as: E.L. Regner, et al., Biochemical characterization of thioredoxin reductase from *Babesia bovis*, Biochimie (2013), http://dx.doi.org/10.1016/j.biochi.2013.11.002

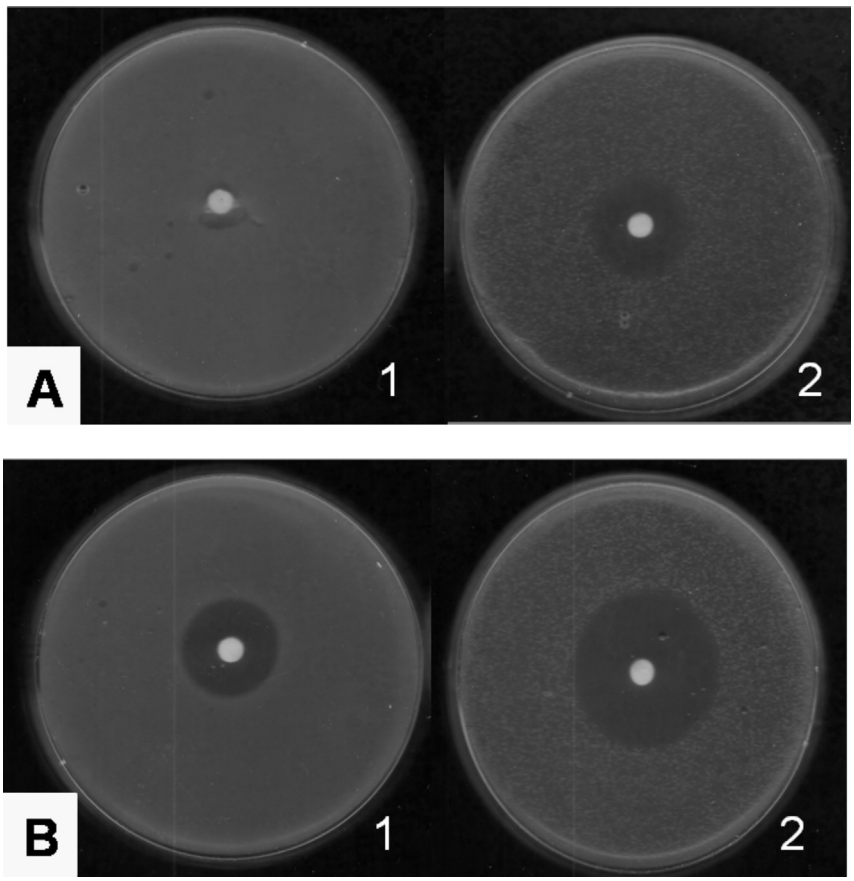

Fig. 3. Disk inhibition assays for growing of transformed *E. coli* in presence of diamide. *E. coli* cells transformed with **(1)** the pET28/*Bbo*TrxRΔ50N vector or with **(2)** the pET28 plasmid (control assay) were exposed to A: 20 mM diamide or B: 200 mM diamide. The differences between control and *Bbo*TrxRΔ50N transformed cells were reliable after repetition in three independent experiences.

of mammalian [31] and malarial Trx systems [20]. To evaluate the catalytic behavior of GSSG/GSNO reduction by either *Bbo*Trx or *Bbo*TrxR, the second order rate constant for this reaction (k'') was calculated according to the following equation:

$$v = k'' \cdot [A] \cdot [B]$$

where [A] is the initial concentration of Trx_{Red} or $TrxR_{Red}$, [B] is the initial GSSG or GSNO concentration and k'' is the second order rate constant of the reaction. We found that GSNO is a substrate of *Bbo*TrxR (Table 2), being the enzyme capacity for GSNO-reduction ($k'' = 461\ M^{-1}\ s^{-1}$) comparable with those parameters calculated for other H-TrxRs (i.e. *P. falciparum*, $10^3\ M^{-1}\ s^{-1}$; and calf thymus, $10^5\ M^{-1}\ s^{-1}$) [31,33]. In contrast, GSSG was a very poor substrate of *Bbo*TrxR (Table 2), which is in agreement with that reported for TrxRs from other species [31,33]. Additionally, we investigated the capacity of *Bbo*Trx to reduce GSSG (Fig. 8A) and GSNO (Fig. 8B). When the reaction mixture containing reduced *Bbo*Trx (in presence

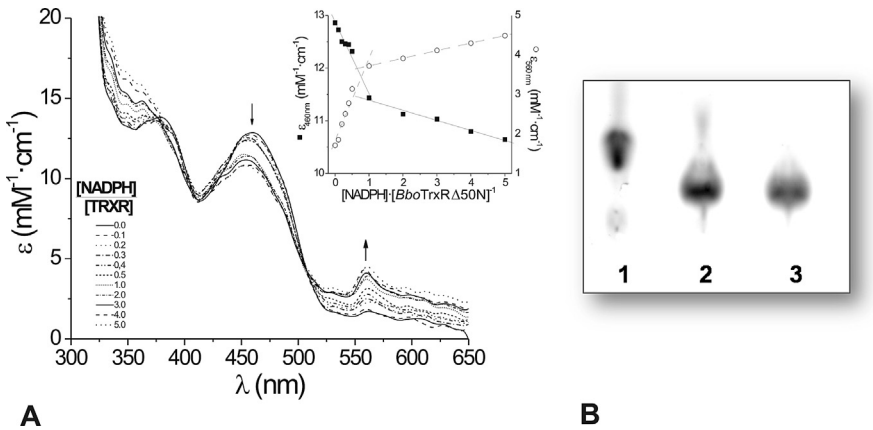

Fig. 4. UV–visible absorption spectra of *Bbo*TrxRΔ50N and identification of the flavin as FAD by thin layer chromatography. A – Redox titration of *Bbo*TrxRΔ50N with different NADPH equivalents. The titration was conducted aerobically at 25 °C, in 100 mM phosphate buffer, pH 8.0. *Bbo*TrxRΔ50N was at a final concentration of 12 μM. Inset: The changes in ε at 460 nm and 560 nm during the titration with NADPH. B – Determination of flavin by thin layer chromatography. Chromatography was revealed by fluorescence with the *Typhoon* scanner. *Lane 1*, FMN commercial standard; *lane 2*, supernatant obtained after heat treatment of purified *Bbo*TrxRΔ50N and *lane 3*, FAD commercial standard.

Please cite this article in press as: E.L. Regner, et al., Biochemical characterization of thioredoxin reductase from *Babesia bovis*, Biochimie (2013), http://dx.doi.org/10.1016/j.biochi.2013.11.002

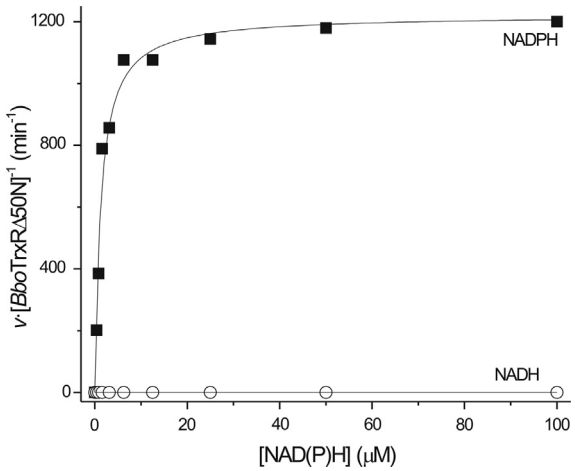

Fig. 5. Kinetic of NAD(P)H oxidation by *Bbo*TrxR. The reactions were monitored with the *Bbo*Trx-mediated reduction of DTNB (at 405 nm) with 500 μM DTNB, 20 μM *Bbo*Trx, 18 nM *Bbo*TrxR and NADPH or NADH (up to 100 μM) at pH 8.0 and 30 °C.

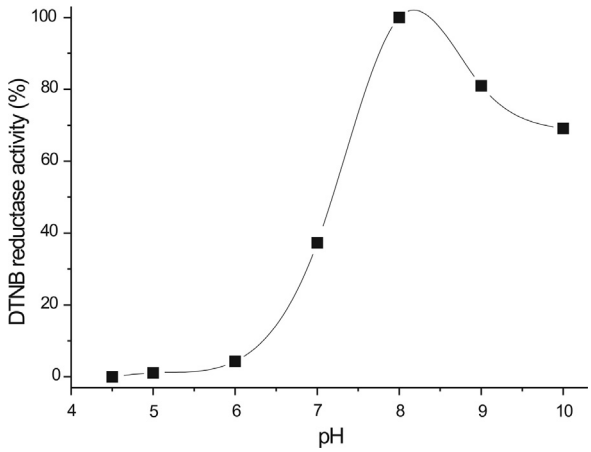

Fig. 7. pH-dependent activity profile of *Bbo*TrxRΔ50N for DTNB reductase activity. Assays were performed at 30 °C in 100 mM potassium phosphate at different pH values with 0.1 mM NADPH, 2.5 mM DTNB, and 18 nM *Bbo*TrxRΔ50N. The calculated optimal pH value was 8.0. The calculated value is the mean of at least three independent sets of data.

of NADPH and *Bbo*TrxR) was supplemented with GSNO or GSSG, the NADPH oxidation rates was increased proportionally to *Bbo*Trx and GSNO/GSSG concentrations. The calculated kinetic constants are presented in Table 2. The above results indicate that GSNO and GSSG can be directly reduced by *Bbo*Trx. Although an *in silico* analysis of the *B. bovis* genome fails in finding a gene encoding for a glutathione reductase, we identified genes encoding for enzymes involved in the glutathione metabolism (specifically glutathione synthetase and glutathione *S*-transferase). Thus, the overall picture suggests the occurrence of this key antioxidant thiol in the parasite, being Trx involved in reducing GSSG *in vivo*. A similar redox metabolism has been described in other organisms, like in *Drosophila melanogaster*, which lacks glutathione reductase and has the Trx system mainly involved in maintaining the levels of GSH [34].

3.4. Inhibition studies of BboTrxR

The disulfide reductase activity of *Bbo*TrxR was sensitive to low concentrations (<10 μM) of Cu^{2+} and Zn^{2+}, with IC_{50} values for the respective divalent cation determined in 0.84 ± 0.05 μM and 4.0 ± 0.7 μM. These results support the established mechanism involving cysteine residues in the disulfide reductase activity of this enzyme. Moreover, we evaluated the inhibitory capacity of $NADP^+$ on the NADPH-dependent disulfide reductase activity exhibited by *Bbo*TrxR using DTNB. At fixed concentration of DTNB and varied of NADPH, $NADP^+$ acted as a competitive inhibitor with respect to the substrate with an inhibition constant (K_i) of 80 μM, obtained after Dixon plots [19] (Fig. 9).

In addition, we investigated the effect of 4,5-dibromo-2,7-dinitrofluorescein, a red dye commonly known as Eosin B, which has been reported to inhibit *P. falciparum* TrxR and to exhibit antimalarial activity [35]. Eosin B was evaluated as a potential inhibitor of the disulfide reductase activity of *Bbo*TrxR (Fig. 10). Our data suggest that Eosin B behaves itself as a partial mixed inhibitor of the enzyme assayed with DTNB as substrate (Fig. 10A). The inhibition analysis (Fig. 10B) showed a hyperbolic profile in regard to k_{cat} ($K_{iu} = 1.8 \pm 0.2$ μM) and a linear inhibition behavior concerning Km ($K_{ic} = 60 \pm 8$ μM). Altogether, our results are of value for a potential use of TrxR as a molecular target for development of drugs for bovine babesiosis treatment.

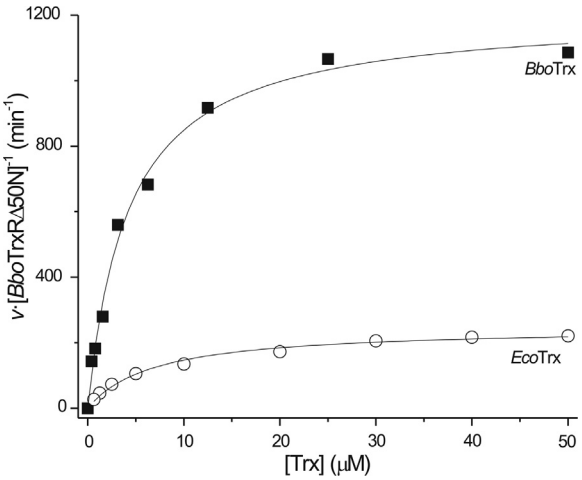

Fig. 6. Kinetic behavior of TrxR from *B. bovis*. TRX-reduction kinetics by *Bbo*TrxRΔ50N assayed in presence of (■) *Bbo*Trx or (○) *Eco*Trx. Trx-reduction was measured by monitoring NADPH oxidation at 340 nm with 0.1 mM NADPH, 0.1 mM human insulin, 0.4–50 μM Trxs, and 18 nM *Bbo*TrxRΔ50N at pH 8.0 and 30 °C.

4. Discussion

In general, the Trx system plays an important role in parasitic microorganisms, mainly for the cell defense against ROS and/or RNS. In apicomplexan protozoa the system functioning is critical during the erythrocytic stage, where the toxic effects of ROS and RNS become more relevant. In this work we describe the biochemical properties of protein members of the Trx system from the bovine parasite *B. bovis*. To the best of our knowledge, this is the

Table 1
Kinetic parameters of *Bbo*TrxRΔ50N at pH 8.0 and 30 °C.

Cosubstrate	Substrate	Km (μM)	k_{cat} (min^{-1})	$k_{cat}·Km^{-1}$ (M^{-1} s^{-1})
*Bbo*Trx 20 μM	NADH	No substrate		
	NADPH	1.3 ± 0.2	1200 ± 22	$1.5·10^7$
NADPH 100 μM	DTNB	238 ± 31	650 ± 1	$4.5·10^3$
	*Bbo*Trx	4.2 ± 0.4	1208 ± 38	$4.8·10^6$
	*Eco*Trx	7.0 ± 0.8	247 ± 8	$6.0·10^5$

Please cite this article in press as: E.L. Regner, et al., Biochemical characterization of thioredoxin reductase from *Babesia bovis*, Biochimie (2013), http://dx.doi.org/10.1016/j.biochi.2013.11.002

Table 2
Kinetic constant values for reduction of GSNO and GSSG by *Bbo*TrxR/*Bbo*Trx system at pH 8.0 and 30 °C.

Substrate	k'' (M^{-1} s^{-1})	
	*Bbo*Trx[a]	*Bbo*TrxRΔ50N[b]
GSSG	173 ± 1	<1
GSNO	90 ± 2	461 ± 12

[a] GSNO or GSSG reduction (7.25–1000 μM) was assayed with 1 μM *Bbo*TrxRΔ50N, 0.1 mM NADPH, and different concentrations (1–8 μM) of *Bbo*Trx.
[b] GSNO or GSSG reduction (7.25–1000 μM) was assayed with 0.01–1 μM *Bbo*TrxRΔ50N and 0.1 mM NADPH. The reactions were started by adding GSNO or GSSG. This assay was followed by the absorbance decrease at 340 nm.

first characterization of *Bbo*TrxR activity and functionality. Biochemical results indicate that *Bbo*TrxR is a homodimeric NADPH-dependent disulphide oxidoreductase that possesses FAD as cofactor, similar to other TrxRs [36,37]. *In silico* analysis points out that the *Bbo*TrxR belongs to the H-TrxR group, exhibiting a second pair of redox-active residues in its C-terminal region [36,37]. In the case of mammalian TrxR, the C-terminal redox-active center comprises vicinal selenocysteine–cysteine residues (SeCys-Cys), whereas *Bbo*TrxR contains a CXXXXC motif instead [36–38]. Strikingly, we found that the *Bbo*TrxR/*Bbo*Trx system shares several features with its ortholog in *P. falciparum*; such as the kinetic and physical properties exhibited by *Bbo*TrxR and the capacity for reducing GSNO and GSSG. This latter capacity would be of high relevance, since *B. bovis* lacks a putative specific reductase for GSSG and because GSH is the most abundant intracellular non-protein thiol of key involvement in redox homeostasis. Our data suggest that the antioxidant defense in *B. bovis* is supported by the *Bbo*TrxR/*Bbo*Trx system.

Assays of resistance to oxidative damage performed with transformed *E. coli* cells indicate the *in vivo* functionality of the truncated constructed form of *Bbo*TrxR. Our kinetic results suggest that the enzyme would be an important cellular tool for maintaining redox homeostasis in the *B. bovis* living under oxidative conditions. The possibility for this functional relevance is tempered by the supposed mitochondrial localization of the enzyme predicted from the coding gene. However, it is worth to consider two issues: (i) the genome of *B. bovis* shows the presence of only one TrxR, and (ii) in the apicomplexan *P. falciparum* glutathione reductase is coded by a single gene and exhibits a dual localization (mitochondrial and cytoplasmic) after an alternative translation initiation [39]. Thus, this latter could also be the case for the occurrence of TrxR in *B. bovis*. Besides, we found that Eosin B is an

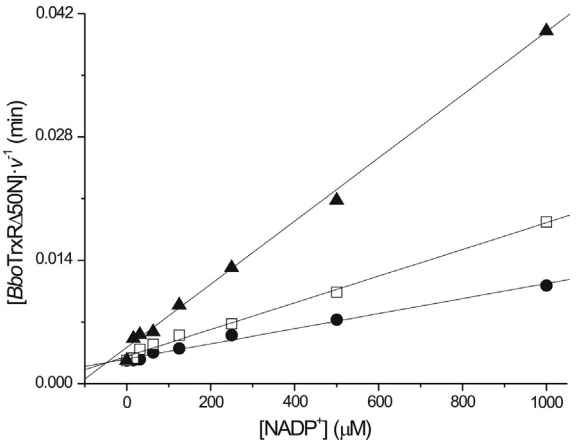

Fig. 9. Dixon plot for $NADP^+$-mediated inhibition of disulfide reductase activity of *Bbo*TrxRΔ50N. The assays were performed in presence of different concentrations of $NADP^+$ (7.25–1000 μM) at different NADPH concentrations: (▲) 12.5; (□) 25; and (●) 50 μM with 18 nM *Bbo*TrxRΔ50N and 2.5 mM DTNB at 30 °C and pH 8.0.

inhibitor of the disulfide reductase activity exhibited by *Bbo*TrxR, with values of inhibition constants giving potential utility to the dye for its use as a drug targeted to the enzyme. In this way, it might be of value to study (in the near future) the effect of the dye on *B. bovis* cultures. Finally, it is worth to point out that this is the first report about identification, molecular cloning and functional characterization of the *Bbo*TrxR/*Bbo*Trx system. Control of the redox balance in the cell is considered as one of the most important biological properties for parasites living in oxygen-rich environments such as erythrocytes [23]. The present work contributes with key information for future design studies to generate and validate new procedures for babesiosis therapy and/or prevention based on attacking the antioxidant capacity of the parasite.

5. Conclusion

We present the molecular cloning, recombinant expression, and characterization of the kinetic and structural properties of thioredoxin reductase from *B. bovis*. The purified recombinant enzyme presented NADPH-dependent disulfide reductase activity with the model substrate DTNB and classic Trx from *B. bovis* and *E. coli*. In addition, the *Bbo*TrxR/*Bbo*Trx system exhibited capacity to reduce GSSG and GSNO, suggesting that the antioxidant defense in *B. bovis*

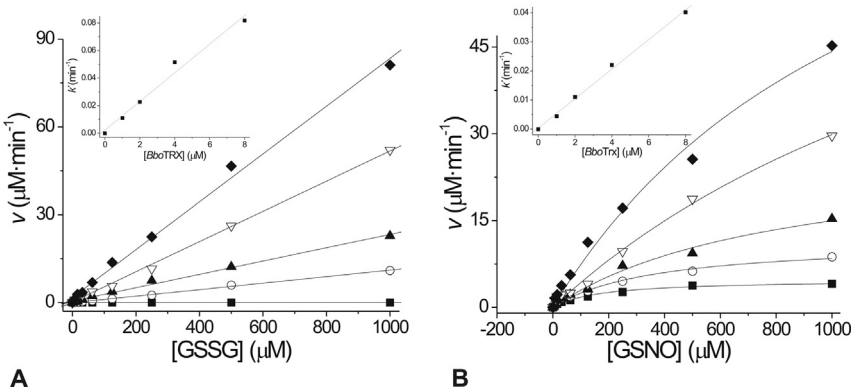

Fig. 8. Trx-dependent GSSG or GSNO reduction kinetics. The assays were performed in presence of different concentrations (7.25–1000 μM) of GSSG (A) or GSNO (B) and *Bbo*Trx: (■) 0; (○) 1; (▲) 2; (▽) 4 and (◆) 8 μM with 1 μM *Bbo*TrxRΔ50N and 0.1 mM NADPH at 30 °C and pH 8.0. Inset: Pseudo-first order rate constants (calculated from the slopes of the first graph) vs [*Bbo*Trx].

Please cite this article in press as: E.L. Regner, et al., Biochemical characterization of thioredoxin reductase from *Babesia bovis*, Biochimie (2013), http://dx.doi.org/10.1016/j.biochi.2013.11.002

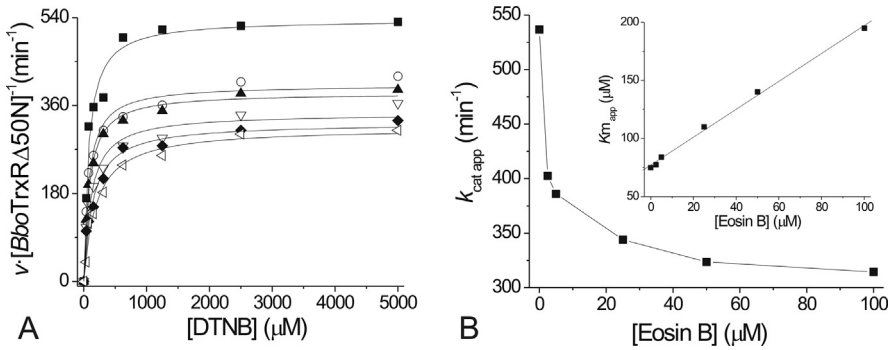

Fig. 10. Eosin B as inhibitor of disulfide reductase activity of *Bbo*TrxRΔ50N. A – Influence of Eosin B upon the DTNB reductase activity. Assays were performed at fixed concentration of NADPH of 100 μM and varied Eosin B concentrations (■) 0; (○) 2.5; (7) 5; (▽) 25; (◆) 50 and (▲) 100 μM. B – Effect of inhibitor upon k_{cat} and *K*m (inset). Eosin B acts as partial mixed inhibitor for DTNB reductase activity of *Bbo*TrxRΔ50N, under the conditions assayed.

could be supported by the *Bbo*TrxR/*Bbo*Trx system. Besides the relevance that the latter could have for the parasite antioxidant defense, to the best of our knowledge this is the first report uncovering the occurrence of these proteins in this parasite.

Acknowledgments

This work was supported by grants from UNL (CAI + D Orientados & Redes), CONICET (PIP112-2011-0100439, PIP114-2011-0100168) and ANPCyT (PICT2008-1754, PICT2012-2439). DGA, AAI and SAG are investigator career members from CONICET. CST is investigator from INTA.

References

[1] R. Bock, L. Jackson, A. De Vos, W. Jorgensen, Babesiosis of cattle, Parasitology 129 (2004) 247–269.
[2] M.T. Allsopp, T. Cavalier-Smith, D.T. De Waal, B.A. Allsopp, Phylogeny and evolution of the piroplasms, Parasitology 108 (1994) 147–152.
[3] S. Müller, R.D. Walter, R.L. Krauth-Siegel, Thiol-based redox metabolism of protozoan parasites, Trends Parasitol. 19 (2003) 320–328.
[4] K. Becker, S. Gromer, H.R. Schirmer, S. Müller, Thioredoxin reductase as a pathophysiological factor and drug target, Eur. J. Biochem. 267 (2000) 6118–6125.
[5] K.A. Brayton, D.R. Herndon, L. Hannick, L.S. Kappmeyer, S.J. Berens, S.L. Bidwell, W.C. Brown, J. Crabtree, D. Fadrosh, T. Feldblum, H.A. Forberger, B.J. Haas, J.M. Howell, H. Khouri, H. Koo, D.J. Mann, J. Norimine, I.T. Paulsen, D. Radune, Q. Ren, R.K. Smith Jr., C.E. Suarez, O. White, J.R. Wortman, D.P. Knowles Jr., T.F. McElwain, V.M. Nene, Genome sequence of *Babesia bovis* and comparative analysis of apicomplexan hemoprotozoa, Plos Pathog. 3 (2007) 1401–1413.
[6] J. Nordberg, E. Arnér, Reactive oxygen species, antioxidants, and the mammalian thioredoxin system, Free Rad. Biol. Med. 31 (2001) 1287–1312.
[7] E. Arnér, A. Holmgren, Physiological functions of thioredoxin and thioredoxin reductase, Eur. J. Biochem. 267 (2000) 6102–6109.
[8] D. Mustacich, G. Powis, Thioredoxin reductase, Biochem. J. 346 (2000) 1–8.
[9] C.H. Williams, L.D. Arscott, S. Muller, B.W. Lennon, M.L. Ludwig, P.F. Wang, D.M. Veine, K. Becker, R.H. Schirmer, Thioredoxin reductase: two modes of catalysis have evolved, Eur. J. Biochem. 267 (2000) 6110–6117.
[10] M. Kohárýová, Oxidative stress and thioredoxin system, Gen. Physiol. Biophys. 27 (2008) 71–84.
[11] C. Nickel, S. Rahlfs, M. Deponte, S. Koncarevic, K. Becker, Thioredoxin networks in the malarial parasite plasmodium falciparum, Antioxid. Redox Signal. 8 (2006) 1227–1239.
[12] S. Kawazua, H. Okud, S. Kanob, Peroxiredoxins in malaria parasites: parasitologic aspects, Parasitol. Int. 57 (2008) 1–7.
[13] M. Tanaka, T. Sakurai, N. Yokoyama, N. Inoue, S. Kawazu, Cloning and characterization of peroxiredoxin in *Babesia bovis*, Parasitol. Res. 105 (2009) 1473–1477.
[14] M.P. Gordge, A.A. Noronha-Dutra, Evidence for a cyclic GMP-independent mechanism in the anti-platelet action of *S*-nitrosoglutathione, Br. J. Pharmacol. 124 (1998) 141–148.
[15] M.E. Baravalle, C. Thompson, B. Valentini, M. Ferreira, S. Torioni de Echaide, M.F. Christensen, I. Echaide, *Babesia bovis* biological clones and the inter-strain allelic diversity of the Bv80 gene support subpopulation selection as a mechanism involved in the attenuation of two virulent isolates, Vet. Parasitol. 190 (2012) 391–400.
[16] U.K. Laemmli, Cleavage of structural proteins during the assembly of the head of bacteriophage T4, Nature 227 (1970) 680–685.
[17] M.M. Bradford, A rapid and sensitive method for the quantitation of microgram quantities of protein utilizing the principle of protein-dye binding, Anal. Biochem. 72 (1976) 248–254.
[18] L. Ledesma García, E. Rivas-Marín, B. Floriano, R. Bernhardt, K. Ewen, F. Reyes-Ramírez, E. Santero, ThnY is a ferredoxin reductase-like iron-sulfur flavoprotein that has evolved to function as a regulator of tetralin biodegradation gene expression, J. Biol. Chem. 286 (2011) 1709–1718.
[19] M. Dixon, The determination of enzyme inhibitor constants, Biochem. J. 55 (1953) 170–171.
[20] S.M. Kanzok, R.H. Schirmer, I. Türbachova, R. Iozef, K. Becker, The thioredoxin system of the malaria parasite *Plasmodium falciparum* glutathione reduction revisited, J. Biol. Chem. 275 (2000) 40180–40186.
[21] S.M. Kanzok, S. Rahlfs, K. Becker, R.H. Schirmer, Thioredoxin, thioredoxin reductase, and thioredoxin peroxidase of malaria parasite *Plasmodium falciparum*, Methods Enzymol. 347 (2002) 370–381.
[22] A. Holmgren, Bovine thioredoxin system. Purification of thioredoxin reductase from calf liver and thymus and studies of its function in disulfide reduction, J. Biol. Chem. 252 (1977) 4600–4666.
[23] S. Müller, Redox and antioxidant systems of the malaria parasite *Plasmodium falciparum*, Mol. Microbiol. 53 (2004) 1291–1305.
[24] P. Ghezzi, B. Romines, M. Fratelli, I. Eberini, E. Gianazza, S. Casagrande, T. Laragione, M. Mengozzi, L.A. Herzenberg, L.A. Herzenberg, Protein glutathionylation: coupling and uncoupling of glutathione to protein thiol groups in lymphocytes under oxidative stress and HIV infection, Mol. Immunol. 38 (2001) 773–780.
[25] E. Arnér, L. Zhong, A. Holmgren, Preparation and assay of mammalian thioredoxin and thioredoxin reductase, Methods Enzymol. 300 (1999) 226–239.
[26] Z. Cheng, L.D. Arscott, D.P. Ballou, C.H. Williams, The relationship of the redox potentials of thioredoxin and thioredoxin reductase from *Drosophila melanogaster* to the enzymatic mechanism: reduced thioredoxin is the reductant of glutathione in *Drosophila*, Biochemistry 46 (2007) 7875–7885.
[27] N. Cenas, H. Nivinskas, Z. Anusevicius, J. Sarlauskas, F. Lederer, E.S. Arner, Interactions of quinones with thioredoxin reductase: a challenge to the antioxidant role of the mammalian selenoprotein, J. Biol. Chem. 279 (2004) 2583–2592.
[28] P.J. McMillan, L.D. Arscott, D.P. Ballou, K. Becker, C.H. Williams, S. Muller, Identification of acid-base catalytic residues of high-Mr thioredoxin reductase from *Plasmodium falciparum*, J. Biol. Chem. 281 (2006) 32967–32977.
[29] S. Gromer, L.D. Arscott, C.H. Williams, R.H. Schirmer, K. Becker, Human placenta thioredoxin reductase: isolation of the selenoenzyme, steady state kinetics, and inhibition by therapeutic gold compounds, J. Biol. Chem. 273 (1998) 20096–20101.
[30] M. Luthman, A. Holmgren, Rat liver thioredoxin and thioredoxin reductase: purification and characterization, Biochemistry 26 (1982) 6628–6633.
[31] A. Nikitovic, *S*-Nitrosoglutathione is cleaved by the thioredoxin system with liberation of glutathione and redox regulating nitric oxide, J. Biol. Chem. 271 (1996) 19180–19185.
[32] L. Zhong, A. Holmgren, Essential role of selenium in the catalytic activities of mammalian thioredoxin reductase revealed by characterization of recombinant enzymes with selenocysteine mutations, J. Biol. Chem. 275 (2000) 18121–18128.
[33] R. Attarian, C. Bennie, H. Bach, Y. Av-Gay, Glutathione disulfide and *S*-nitrosoglutathione detoxification by *Mycobacterium tuberculosis* thioredoxin system, FEBS Lett. 583 (2009) 3215–3220.
[34] S.M. Kanzok, A. Fechner, H. Bauer, J.K. Ulschmid, H.M. Müller, J. Botella-Muñoz, S. Schneuwly, R.H. Schirmer, K. Becker, Substitution of the thioredoxin

system for glutathione reductase in *Drosophila melanogaster*, Science 291 (2001) 643–646.
[35] K.M. Massimine, M.T. McIntosh, L.T. Doan, C.E. Atreya, S. Gromer, W. Sirawaraporn, D.A. Elliott, K.A. Joiner, R.H. Schirmer, K.S. Anderson, Eosin B as a novel antimalarial agent for drug-resistant *Plasmodium falciparum*, Antimicrob. Agents Chemother. 50 (2006) 3132–3141.
[36] P.F. Wang, L.D. Arscott, T.W. Gilberger, S. Müller, C.H. Williams, Thioredoxin reductase from *Plasmodium falciparum*: evidence for interaction between the C-terminal cysteine residues and the active site disulfide-dithiol, Biochemistry 38 (1999) 3187–3196.
[37] T.W. Gilberger, B. Bergmann, R.D. Walter, S. Müller, The role of the C-terminus for catalysis of the large thioredoxin reductase from *Plasmodium falciparum*, FEBS Lett. 425 (1998) 407–410.
[38] T. Tamura, T.C. Stadtman, Mammalian thioredoxin reductases, Methods Enzymol. 347 (2002) 297–306.
[39] S. Kehr, N. Sturm, S. Rahlfs, J.M. Przyborski, K. Becker, Compartmentation of redox metabolism in malaria parasites, PLoS Pathog. 6 (2010) e1001242.

Please cite this article in press as: E.L. Regner, et al., Biochemical characterization of thioredoxin reductase from *Babesia bovis*, Biochimie (2013), http://dx.doi.org/10.1016/j.biochi.2013.11.002